Arabian Journal for Science and Engineering (2019) 44:5107–5116
https://doi.org/10.1007/s13369-018-03716-3

RESEARCH ARTICLE - CIVIL ENGINEERING

Field Study on the Soil Water Characteristics of Shallow Layers on Red Clay Slopes and Its Application in Stability Analysis

Yonghui Chen[1,2] · Bingyi Li[1,2] · Yuntao Xu[3] · Yunpeng Zhao[4] · Jie Xu[1,2]

Received: 31 July 2018 / Accepted: 31 December 2018 / Published online: 7 January 2019

Abstract
Red clay is widely distributed in Zhejiang Province, China. Rain-induced shallow landslides easily occur on red clay slopes due to the reduction in shear strength caused by rainwater infiltration. The aim of this paper was to study the soil–water characteristic of red clay and its application on analyzing the stability of red clay slope. A series of field tests at different depths of red clay slope were carried out to monitor the variations of water content and matric suction under typical climate conditions. The results showed that the distribution of water content in red clay slope is complex because of long-term wetting–drying cycles. The water content within shallow layer is sensitive to external environment, and the response time of the water content is related to rainfall intensity. It is also observed that the soil water characteristic curve (SWCC) varies at different depths. The SWCCs of red clay can be fitted by linear function. The SWCCs from laboratory tests illustrated that saturated water content is more than 40%. Most of the SWCCs obtained at the depth of 90 cm are within the hysteresis loops of the SWCCs from laboratory test. The short-term rainfall has less effect on the stability of the slope, but the stability continuously decreases after the rain stops. The SWCCs obtained from laboratory were applied to analyze slope stability. Considering the influence of cracks, the computed results are close to field data. The study has a certain directive significance to the design of red clay slopes.

Keywords Slope stability · Red clay · Rainfall infiltration · Matric suction · Water content · Soil water characteristic curve (SWCC)

1 Introduction

Landslides can be caused by many factors such as morphology, geology, soil origin. In some mountainous area of southeast China, landslides often occur during the summer or fall, especially after rainy days. Water infiltration during rainfall is a significant issue when designing and protecting infrastructure slopes in expressways and water conservancy projects. Numerous studies have been conducted to illustrate the effect of rainfall infiltration on slopes [1–3]. The reduction in matric suction is a major cause of the instability of unsaturated soil slopes [4–6].

There are various methods to evaluate the stability of slopes during or after rainfall including numerical simulations [2,7], analytical solutions [2,7–10] and field monitoring [2,7–14]. Numerical studies can be used to simulate the process of infiltration and calculate the factor of safety [7,15]. The parameters obtained through laboratory or in-situ tests are crucial to the numerical analysis and analytical methods in geotechnical engineering [16,17]. Moreover, the data from field monitoring are closer to the real condition, which makes the analysis more accurate and effective [18,19].

Unsaturated soil slopes composed of loess [14,20,21] and expansive soil [22,23] have been studied in field and laboratory. Most of the field tests were only carried out to measure the variation of water content and matric suction. However, few research results were compared with laboratory results and applied into further slope stability analysis. In China, red clay is widely distributed in some mountainous areas.

✉ Bingyi Li
bylee17@163.com

1 Key Laboratory of Geomechanics and Embankment of Ministry of Education, Geotechnical Research Institute, Hohai University, Nanjing 210098, China

2 Jiangsu Research Center for Geotechnical Engineering Technology, Hohai University, Nanjing 210098, China

3 Zhejiang Province Institute of Communication Planning, Design & Research, Hangzhou 310006, China

4 Department of Civil and Environmental Engineering, University of Maryland, College Park 20742, USA

Red clay usually has high liquid limit and low permeability, which is unfavorable soil for engineering projects according to the related Chinese criterions. Compared to expansive soil, red clay has lower dilatability. Landslides may occur on red clay slopes during rainfall due to its sensitivity to water. Although researchers have demonstrated the characteristics of red clay by laboratory experiments and numerical study [24–26], few field studies on red clay slopes have been conducted. In situ, the infiltration process of water into slope is different from laboratory tests. Furthermore, soil in field is always under complicated condition. And it is difficult to illustrate the stress state under soil layer with various boundary conditions [22,27]. Finally different selections of soil water characteristic curves (SWCCs) are always ignored in the conventional numerical analysis, which causes errors to the assessment of slope stability [28]. In some studies, different soil water characteristic curves were applied into slope analysis [29,30]. However, the data from SWCC curves were based on pore space distribution (PSD) and previous models rather than actual field measurement.

In this paper, the variations of water content and matric suction at different depth of red clay slope were measured during sunny and rainy days. The results are reported and analyzed with an aim of giving an insight into moisture movement and mechanism of rain-induced landslides under rainfall. The SWCCs measured by field monitoring were compared with laboratory tests. Numerical simulation was also conducted to analyze the stability of red clay slopes using SWCCs from both filed monitoring and laboratory test. This study is meaningful for the analysis and design of red clay slope.

2 Field Monitoring

2.1 The Test Site

The test site is located in Lishui, Zhejiang Province, China (Fig. 1), where the Longquan-Pucheng expressway project is under construction. The project is in a mountainous area in the southwest of Zhejiang Province. The average rainfall is 1600 mm per year in the area of the project. In Lishui city, it rains heavily a lot in summers and rains continuously in falls because of the seasonal typhoons. The slopes under research are left and right cutting sides at around the K15 + 560 section of the expressway. The heights of the two slopes are 14.5 m and 15 m respectively. Both slopes are cut into two stages with a step of 2 m width, and the gradients of the upper and lower sections are 1:1.25 and 1:1.1, respectively (Figs. 2, 5a). The soil of the slopes consists mainly of red clay. The physical and mechanical properties of the typical slope soil from previous laboratory experiments are shown in Table 1. Figure 3 shows the particle distribution curve of the

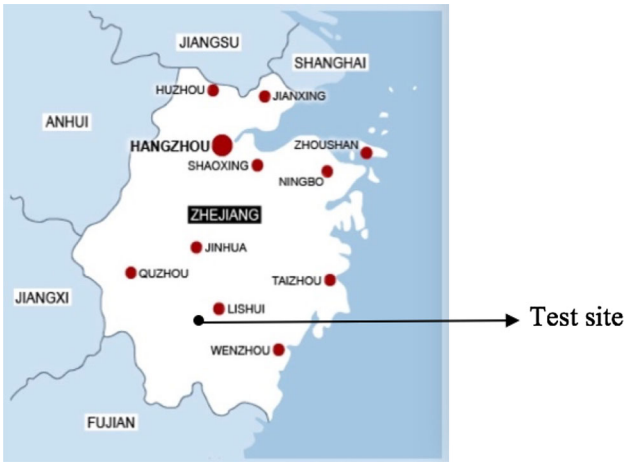

Fig. 1 Site location for the field study

soil in the studied slopes. The measurement of the tests in this paper followed the Chinese Standard for Soil Test Method. According to the Unified Soil Classification System (USCS), the soil in this study was classified as CH.

2.2 Monitoring Instruments and Methods

Field monitoring mainly included volumetric water content, matric suction and rainfall measured by TDR water content sensors, tensiometers and rain gauge, respectively. TDR sensors are labeled as MP306 with a measurement range of 0–100% and accuracy of ±2% (Fig. 4a). And tensiometers are labeled as TEN with a measuring range of 0–100 kPa and accuracy of ±2.5 kPa (Fig. 4b). These instruments were calibrated before the field monitoring. The TDR sensors and tensiometers were set at middle steps of the slopes. The monitoring data were collected once a day. There were two observation periods: November to December, 2014, and August to September, 2015, both of which lasted about 20 days.

Previous studies had reported that soil layers within 3 m would be affected by the common rainfall, while more obvious affect occurs within 1 m [12,17]. Considering the specification of the instrument as well, the TDR sensors and tensiometers were installed at 30 cm, 60 cm and 90 cm below the slope surfaces, and both were at the appropriately same depth of two slopes. The setting location of installed monitoring instruments is shown in Fig. 5. The test points at different depths on the left and right slopes were labeled as L3, L6 and L9 (on left slope) and R3, R6 and R9 (on right slope).

2.3 Monitoring Results

(1) Water content

The variation of the volumetric water content measured at the middle stage of the left slope on November 2014 is shown

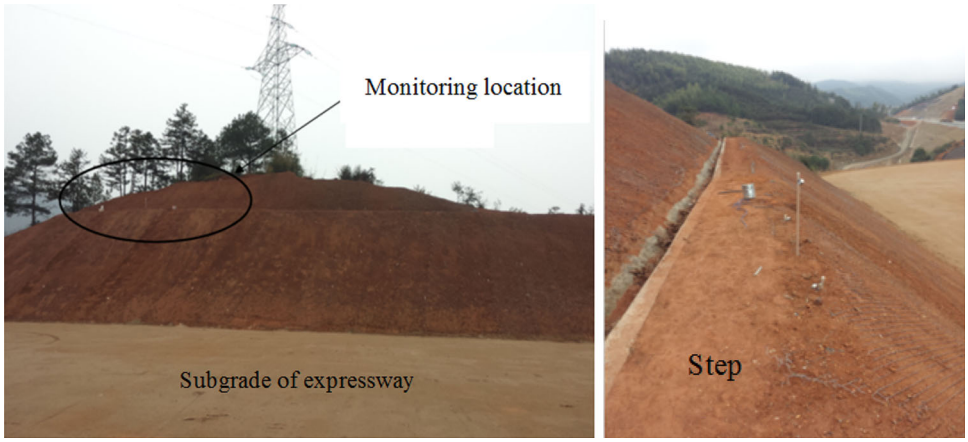

Fig. 2 Photographs of field monitoring on the slope

Table 1 Physical and mechanical properties of slope soil (average values from multiple tests)

Natural water content w (%)	Dry density ρ_d (g/cm^3)	Specific gravity G_s	Void ratio e	Saturation (%)	Free swelling ratio (%)	Liquid limit w_1(%)	Plastic limit w_P(%)	Plasticity index I_P	Saturated permeability coefficient k (cm/s)
35.2	1.28	2.72	1.12	85.1	28	54	28	26	3×10^{-5}

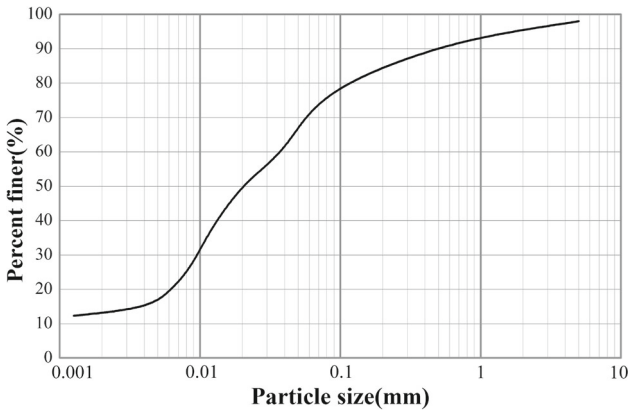

Fig. 3 Particle size distribution curve of red clay

in Fig. 6. Two rounds of rainfall occurred on November 23 and December 6 during the 2014 monitoring period, and the cumulative rainfall was 41.2 mm and 23.2 mm, respectively. According to the meteorological grade, the two rounds of rains belong to heavy and moderate rain, respectively. When there was no rainfall at the site, the moisture changed slightly. Under varied level intensity of sunlight, the water content decreased to different degrees. After the heavy rain, the volumetric water content of the soil at the monitored depth increased rapidly, peaking at about 40%, then decreased gradually. After the moderate rain, the water content increased slightly and then showed a tendency to stabilize.

From August 20 to September 7, 2015, the slope region experienced a number of intermittent rains, and the corresponding rainfall intensity was less than 20 mm/day. The data presented in Fig. 7 indicate that with light rain, the water content of the slope surface fluctuated considerably, while the water content at depths of 30, 60 and 90 cm remained stable or only changed slightly. Because of evaporation, water content of surface even shows decline after rain. The water content increased after the rain lasted a few days, especially at deeper positions under the surface of the slopes.

The data also revealed that the water content had no significant relationship with the depth, because the initial moisture had been affected by a complex co-action of early rainfall and evaporation. However, the depth contributes to the change of water content under conditions of rainfall and evaporation. Under precipitation condition, the water content at shallower positions was higher than that at deeper positions. Additionally, the water content of shallower layers decreased less than that of deeper layers. At the same time, the decrease in water content seems to be more rapid when the rainfall intensity was more than 40 mm/day, while the increase process lasted for a long time with lighter rain.

The variations of the soil moisture at different depths after the rainfall on August 28, 2015, are shown in Fig. 8. The horizontal coordinate represents water content at the specific depth. From August 28 to 30, the monitored area received continuous light or moderate rain; the moisture changed from the shallower to the deeper layer. The initial water content (on the morning of August 28, $t = 0$) at slope surface, depth of 0.3 m, 0.6 m and 0.9 m is 21.8%, 25.1%, 36.9% and 24.2%, respectively. Then the specific depth was influenced by rain infiltration. When the value changed, the "wetting front" [31] had arrived or passed the depth. In this case, after continuous

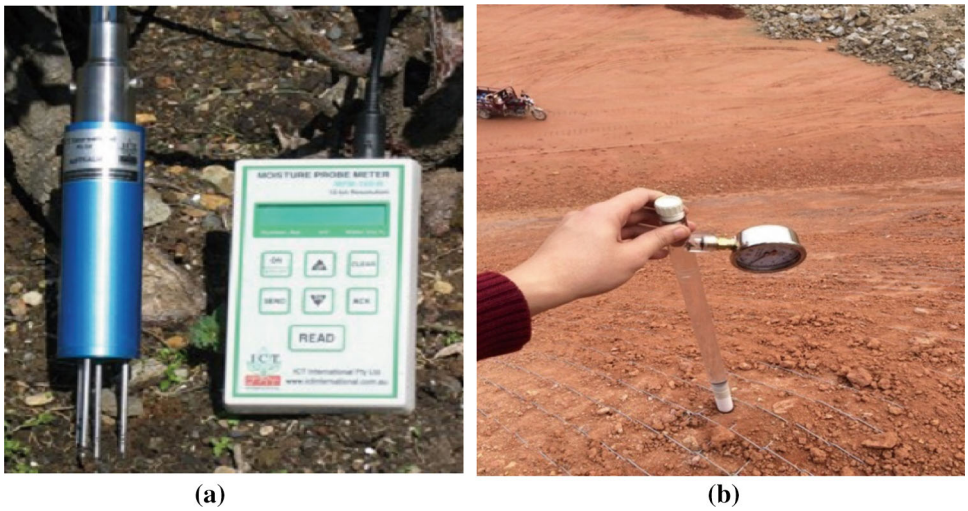

Fig. 4 Monitoring instruments: **a** TDR volumetric water content sensor; **b** tensiometer

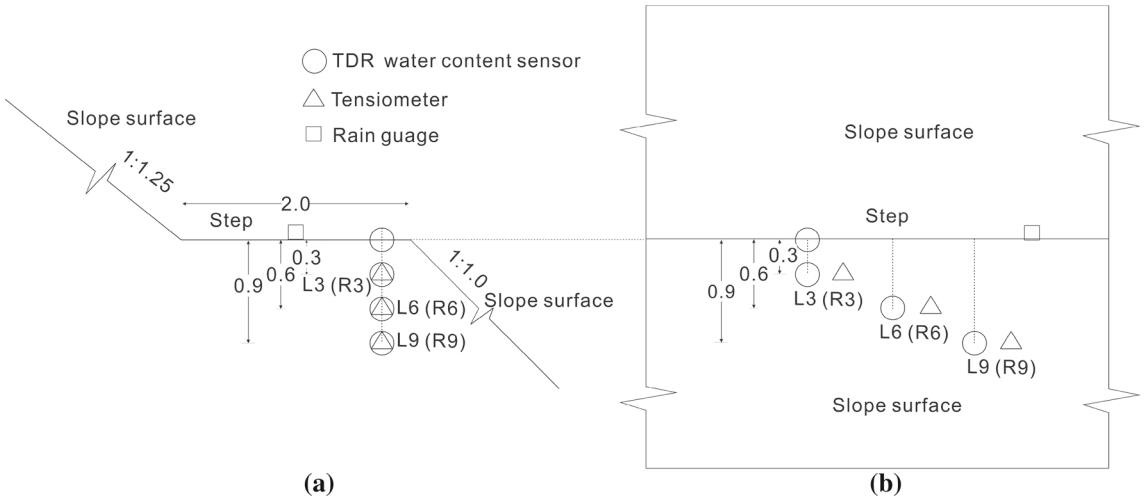

Fig. 5 Layout of monitoring instruments: **a** side profile; **b** front profile (unit: m)

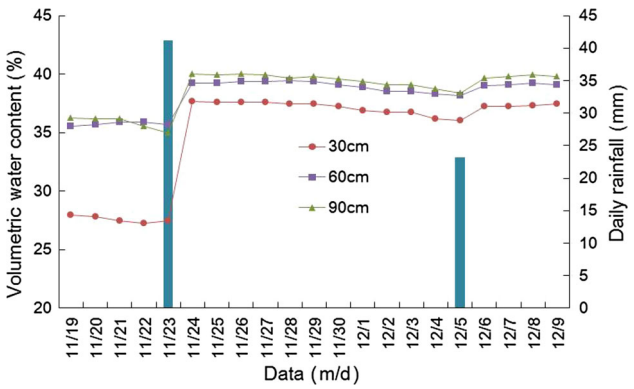

Fig. 6 Variation of volumetric water content of slope from November 19 to December 9, 2014

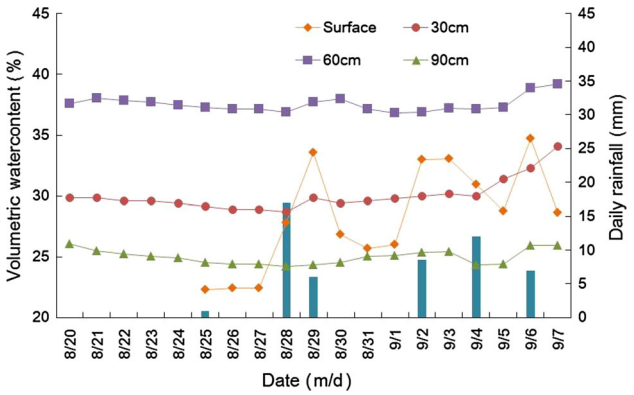

Fig. 7 Variation of volumetric water content of red clay slope from August 20 to September 7, 2015

rain for 7 h, the wetting front had arrived at 30–60 cm below the surface of the slope. And after raining for 32 h, the wetting front arrived at a certain depth between 60 cm and 90 cm. The rain ended on August 30, with the evaporation effect, the moisture of the surface soils decreased gradually from 33.7 to 26.9%, and it occurred later at a further depth of

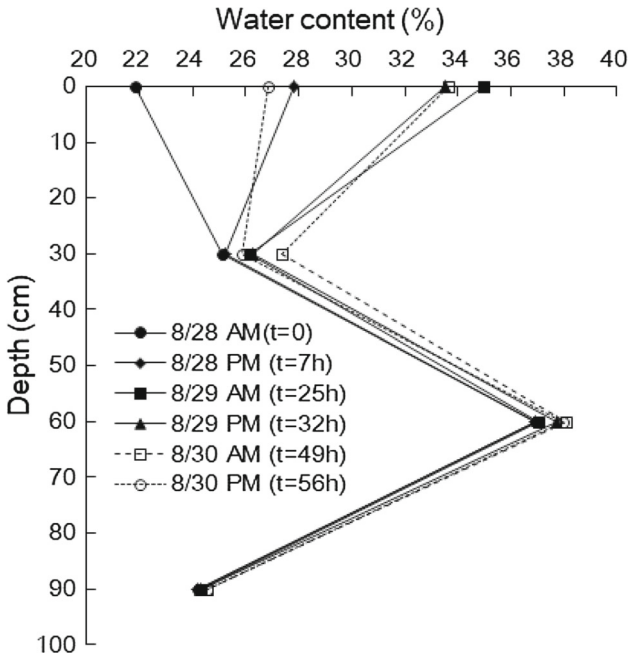

Fig. 8 Variety of water content after rainfall in August 28, 2015

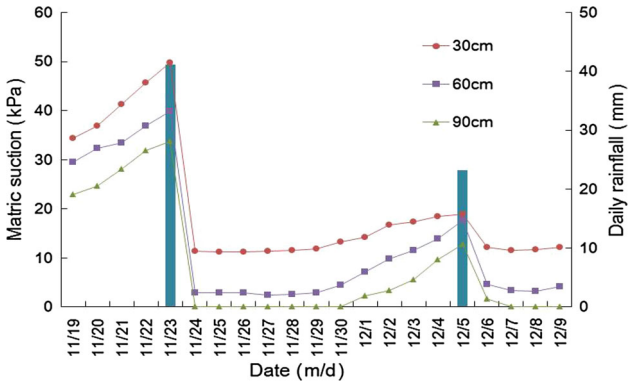

Fig. 9 Variation of the matric suction in the slope from November 19 to December 9, 2014

30 cm. Accordingly, it is evident that there is also a conceptual evaporation front, where moisture would begin to decrease passing this front.

(2) Matric suction

The variation of matric suction with time at different depths in 2014 is shown in Fig. 9. Matric suction dropped when it began to rain, but it started to rise slightly 4 ∼ 5 days after the rain stopped. Water transport was more sensitive during rainfall. The reduction in the matric suction almost showed no response lag. However, when the rain stopped, the suction increased with lag, which is consistent with the changes in moisture wetting and drying of the SWCC detected by laboratory experiments [32]. Overall, matric suction decreased

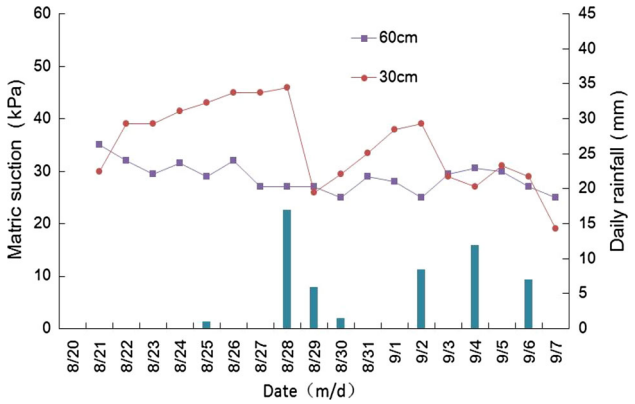

Fig. 10 Variation of the matric suction in the red clay slope from August 20 to September 7, 2015

with the increase of depth. At the depth of 90 cm, the suction was completely lost after the heavy rain, which indicated that the shearing strength of soil at this depth would be less. In the summer of 2015, with continuous light rain, the matric suction measured at the depth of 30 cm and 60 cm fluctuated greatly (Fig. 10).

(3) Field-measured SWCCs

The SWCC, based on the field collected data, was plotted as shown in Fig. 11, where the horizontal and vertical coordinates represent the matric suction and volumetric water content, respectively (data acquired in 2015 are not shown because of their little variation). The field-measured matric suction SWCC mainly ranges from 0 to 60 kPa, and no obvious hysteresis effect was observed. The curves at different depths show various shapes: curves at 30 cm depth are steep, while curves at 60 cm and 90 cm depth are relatively smooth.

It has been found that the shape of the SWCC is related to overburden stress of the soil. The smaller the overburden stress was, the smaller the slope of the curve was. Under a larger overburden stress, the SWCC is smoother and has a greater slope after the point of air entry value. The values measured at depth of 30, 60 and 90 cm, and the overburden stress at each measuring point was approximately 6, 12 and 18 kPa. Thus, the regulation of the field SWCC is the same as that of laboratory tests [32]. Under more vertical stress, soil is compacted into a higher degree, where the void among soil particles is less and more homogeneous. Thus, it is hard for air and water to run into or out of void during the process of transport and the rate of transportation is also at a low level. In another word, shapes of SWCCs can be affected by stress state of soil because the void structure is changed.

Without taking the subsection of SWCC into account, the measured data can be fitted to a linear equation and the results are shown in Table 2. The correlation coefficient r^2 of the 5 test points is greater than 0.90, which indicates that the

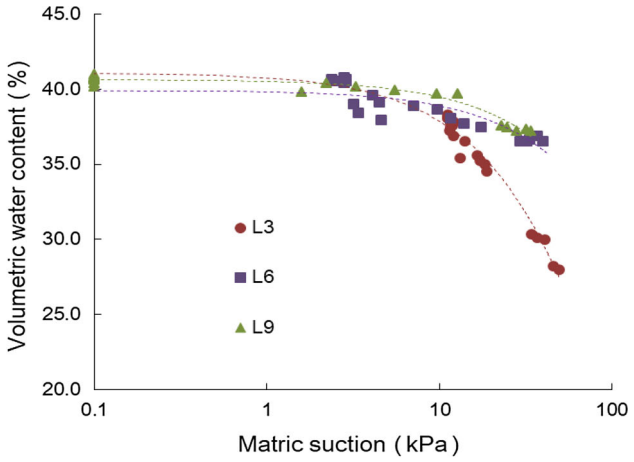

(a) left slope

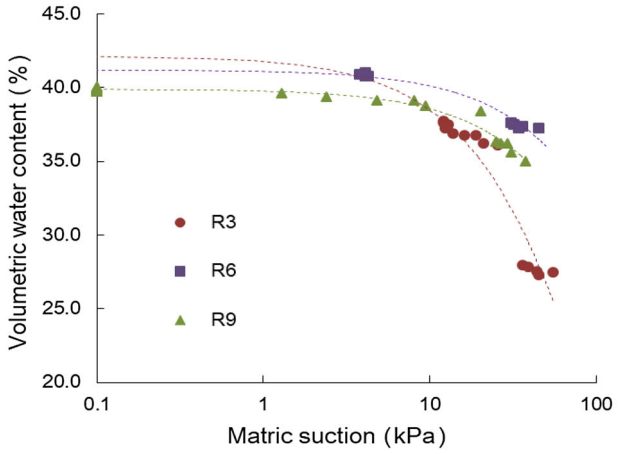

(b) right slope

Fig. 11 Soil–water characteristic curves measured in the field

Table 2 Fitting of SWCCs in the field

Test points	Fitting formula (volumetric water content θ, Matric suction $(u_a - u_w)$)	Correlation coefficient r^2
L3	$\theta = 41.086e^{-0.008(u_a-u_w)}$	0.9745
R3	$\theta = 42.163e^{-0.009(u_a-u_w)}$	0.9224
L6	$\theta = 39.923e^{-0.003(u_a-u_w)}$	0.7561
R6	$\theta = 41.206e^{-0.003(u_a-u_w)}$	0.9670
L9	$\theta = 40.629e^{-0.003(u_a-u_w)}$	0.9519
R9	$\theta = 39.893e^{-0.003(u_a-u_w)}$	0.9659

fitting effect is preferable. The data at 60 cm under the left slope surface did not fit well, probably because there were measurement errors in the matric suction when suction was less than 5 kPa. The first fitting parameter of function can be represented as the saturated water content of the red clay on the slopes, and the second parameter can more directly show the morphology of the SWCCs. In addition, it was revealed in the fitting result that the saturated water content of each depth is around 40%, and the slope varies with the depth.

Fig. 12 FGJ-20 consolidation apparatus on unsaturated red clay

3 Laboratory Test on SWCC

To compare the SWCCs from field monitoring with those form laboratory tests, a few soil specimens were sampled at the monitoring site and brought to the laboratory to conduct tests for the determination of SWCC. The samples were disturbed and reshaped into the same condition as field site.

3.1 Method of Laboratory Test

Laboratory SWCC test was conducted using an FGJ-20 unsaturated soil consolidation apparatus (Fig. 12), which adopts axis translation technique to control the suction of samples. The sample had a diameter of 61.8 mm and a height of 20 mm with a cross-sectional area of 30 cm^2. The test was started after the soil sample is vacuum-saturated. Different suction values were set up in the appropriate order as following: 0.1, 20, 40, 60, 80, 100, 200, 300, 400, 300, 150, 80, 40, 10 and 0.1 kPa, which formed a complete path of moisture drying and wetting. The data were collected when variation of water content was less than 0.02% of sample volume in 24 h at each suction level.

3.2 Test Results

The consolidation tests of the red clay were conducted in the range of 0 ∼ 400 kPa, and the two curves of dehydration and wetting were obtained (Fig. 13). The test results reveal that the air entry value of the drying SWCC was around 20 ∼ 50 kPa, while that of the wetting SWCC was around 1 ∼ 10 kPa. Furthermore, the inflection point appeared at a water content of more than 25%, which is higher than that of other general soils. There was a large gap between the wetting and drying curves, which formed a hysteresis loop.

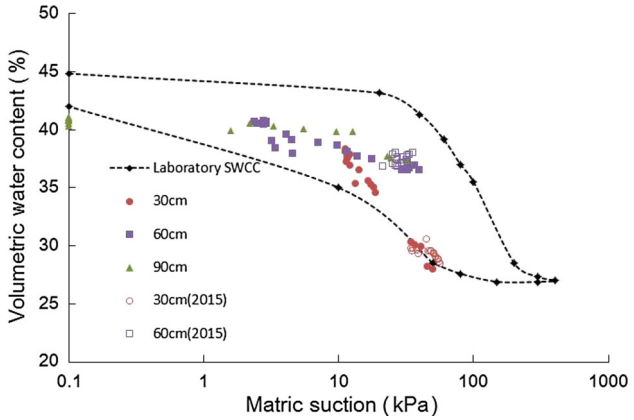

Fig. 13 Comparison of SWCC between field and laboratory test

Field and laboratory SWCCs are plotted in Fig. 13 for comparison, and the following points shall be noted:

(1) It was found that the saturated volumetric water content of red clay is around 40% in both the field and laboratory SWCCs.
(2) There are some differences between the SWCCs obtained from the laboratory tests and field monitoring, but most of field SWCCs are between the moisture wetting curve and the drying curve of the laboratory tests. The shape of the curves is related to the applied stress, and the SWCC measured at the depth of 30 cm is close to that of the laboratory moisture wetting curve without applied load. Meanwhile, it is found that confinement condition is another vital factor [32,33]. In the laboratory tests, soil is completely confined by rigid circular knife, while in-situ soil in shallow layer was considered to be confined by surrounding soil which is a different confinement condition. Because the data were collected in rainy days, the wetting curve was compared with the field curved. Under completely confined condition, laboratory SWCCs show less suction in same water content than field curves, which is consist with results of some other research [34,35].
(3) When the rainfall is less intense (less than 20 mm/day), the water content and matric suction change slightly under the effect of the wet and dry cycles in a short term. When the rainfall is abundant, the water content and the matric suction will change dramatically; thus, the sudden heavy rain and the continuous rainfall will cause adverse safety risks on the red clay slopes.

4 Slope Stability Analysis

The SWCCs obtained from field and laboratory tests were applied to analyze the stability of the unsaturated soil slope.

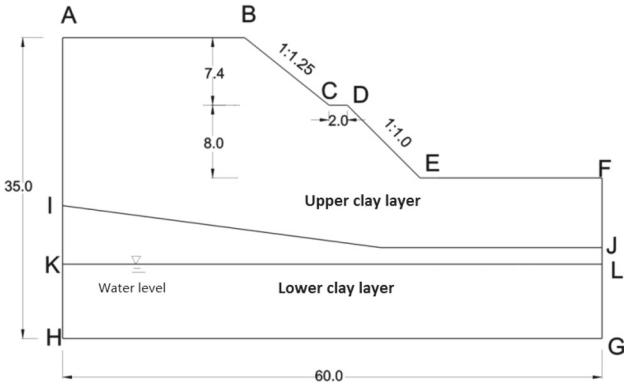

Fig. 14 Calculation model of red clay slope (unit: m)

Table 3 Strength index of the soil layers in the red clay slope

Layers	Effective friction angle φ (°)	Effective cohesion c (kPa)
Upper layer	16.1	23.2
Lower layer	13.3	27.8

The influence of selecting different SWCCs on water distribution and analysis of slope stability is discussed.

4.1 Calculation Model of Slope

The slope of the monitored area was chosen as the calculation model (Fig. 14). The groundwater flows at about 10 m below the foot of the slope. And the strength parameters of the soil layer measured by direct shear tests under saturation condition are shown in Table 3.

Four different SWCCs obtained from the laboratory wetting, drying, field tests at the depths of 90 cm and 30 cm were applied to the slope analysis. It was determined by the variable water pressure head test that the saturated permeability coefficient of the red clay was 3×10^{-5} cm/s. Moreover, according to the permeability coefficient formula proposed by Van Genuchten [36], the relationship between the permeability coefficient and the change of matric suction can be obtained from the SWCCs. Based on the field results and earlier research, the initial volumetric water content was set at 30%.

4.2 Analysis Method

The strength of the unsaturated soil is calculated using the relative mature Fredlund double stress variable strength theory, shown below as:

$$\tau_f = c' + (\sigma_f - u_a)_f \tan\phi' + (u_a - u_w)_f \tan\phi^b \quad (1)$$

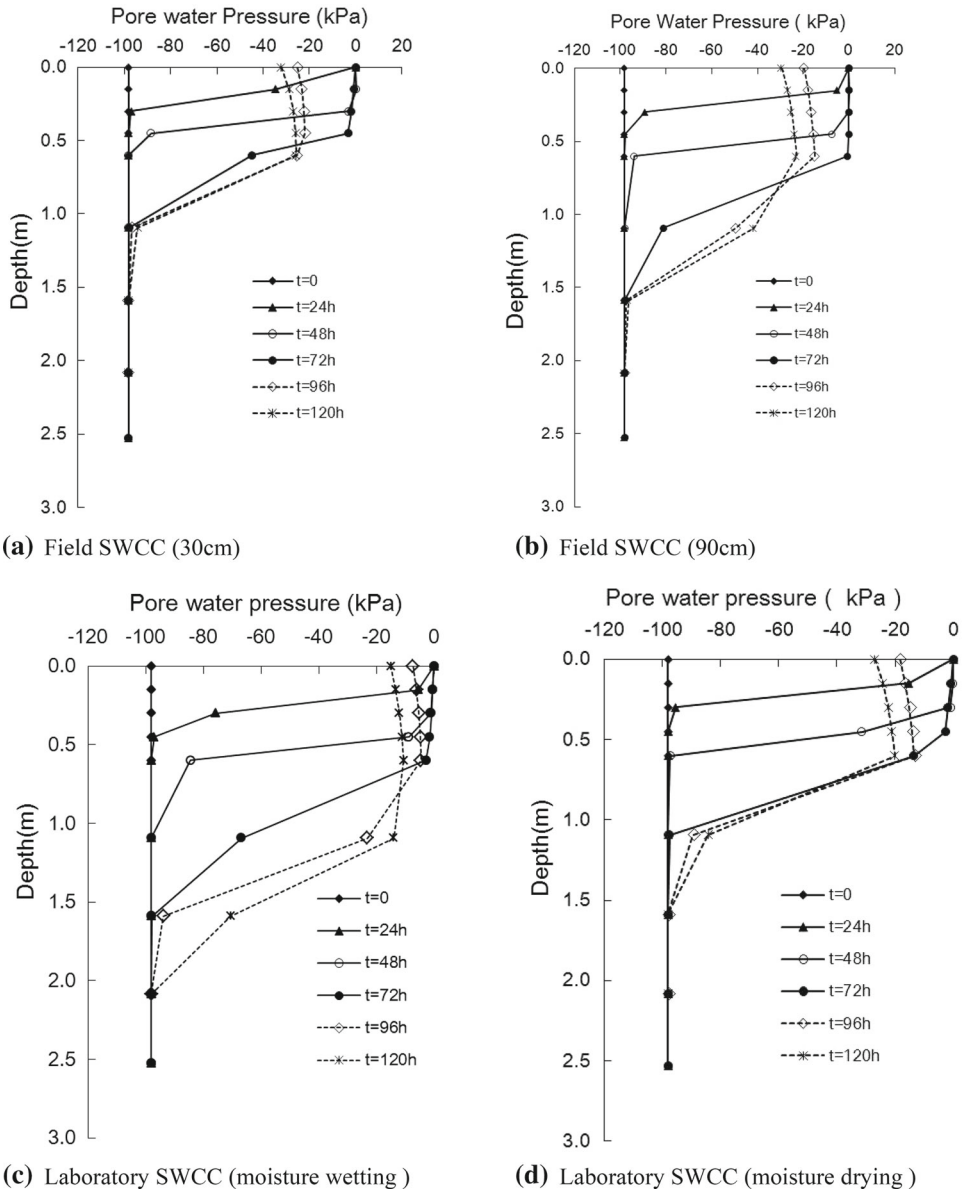

Fig. 15 Variation of pore water pressure in calculation using different SWCCs

(a) Field SWCC (30cm) **(b)** Field SWCC (90cm)

(c) Laboratory SWCC (moisture wetting) **(d)** Laboratory SWCC (moisture drying)

where $(\sigma_f - u_a)_f$ is the normal stress at the destruction surface under condition of failure, $(u_a - u_w)_f$ is the matric suction at the destruction surface when failure occurs, u_a is the pore air pressure at destruction surface when failure, c' is the effective cohesion, φ' is the effective internal friction angle and φ^b is the friction angle associated with suction, simplified by $\varphi^b = 1/2\varphi'$ in this study.

The unsaturated seepage flow field was obtained by the finite element method. The slope rainfall infiltration can be considered as a two-dimensional saturated and unsaturated condition, and the governing equation is as follows:

$$\frac{\partial}{\partial x}\left(k_x \frac{\partial H}{\partial x}\right) + \frac{\partial}{\partial y}\left(k_y \frac{\partial H}{\partial y}\right) + Q = \frac{\partial \theta}{\partial t} \tag{2}$$

where k_x is the permeability coefficient in the x direction, k_y is permeability coefficient in the y direction, H is total head, Q is the seepage flow into the soil, θ is the volumetric water content, and t is the time of process.

Based on the seepage flow field with, the conventional Bishop's divided mesh method combined with the radius of search was applied, the safety factor at most unfavorable face of the slope. The simulated meteorological conditions included a continuous rainfall of 100 mm/day that lasted 3 days and then 2 days of sunny day with evaporation intensity of 7.2 mm/day. When the cracks are considered, the method of setting fractures was referred to previous literature [37]. 1-m deep cracks were set under the surface on the 15-m high slope, with a spacing of 3 m. Under rainfall condition, cracks were filled with water. In other words, the cracks

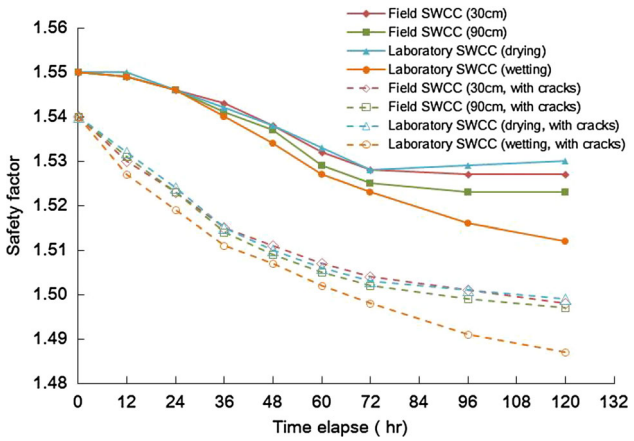

Fig. 16 Variation of safety factor with time elapse using different SWCCs

were set as constant water head boundary, and the water head elevation is slope surface elevation.

The data indicate that with the rainfall infiltration, the pore water pressure changed from shallow to deeper, and the thickness of the saturated layer increases gradually, as depicted in Fig. 15. After 72 h, with the ceasing of the rain and evaporation, the suction of saturated layer starts to increase from shallow to deep, while the water content of deeper layers under the saturated layer keeps rising, which is consistent with the field monitoring results. Accordingly, even when the rainfall ends, the suction in deeper layers of the red clay slope keeps declining, which have adverse effects on the slope. The different distribution of the water content was determined using different SWCCs. However, the thickness of the saturated layer (PWP = 0) is in accordance, around 0.6 m.

4.3 Stability Analysis

The changes of the safety factor based on the seepage field are shown in Fig. 16. Analyzed with the SWCC obtained at 90 cm below the slope surface, the safety factor was smaller than the SWCC obtained at a depth of 30 cm. The result is consistent with the results obtained by laboratory tests [4]. Moreover, when taken into account, the safety factor obtained by the SWCC with more overburden stress is less than that obtained with less or no overburden stress.

Due to the low permeability of red clay, calculated without considering cracks, the safety factor changes little with rainfall, falling from 1.55 to 1.512. Although the overall decline is very little, it can be further used to study the trend of the slope stability during rainfall. In the simulation with field-measured and laboratory-tested SWCCs, the safety factor continues to decrease after the rain has ended. After 96 h (24 h after the rain has stopped), the safety factor calculated with field SWCC is no longer decreased. However, the safety factor calculated with the laboratory SWCC still keeps declining after 120 h, but the trend is obviously decreased. This is because despite the evaporation occurring with the stop of the rain, water still passes down through the pores, which is unfavorable for deeper layers of the red clay slopes and causes a drop in the safety factors. This phenomenon is consistent with the change of the seepage flow field, which also explains the reason that some landslides occur 1–3 days after it stops raining.

From the perspective of the change trend, the simulation with the laboratory moisture wetting curve was similar to the result of the field curve simulation. Under the same conditions, the safety factor calculated with drying curve was smaller, as well as more conservative. To sum up, without field data, it is closer to practical conditions to make the stability analysis of red clay slopes with the laboratory wetting SWCC. However, it is more conservative to choose the drying SWCC. When cracks were considered, the relative change of the stability of the slope was more pronounced and the safety factor dropped from 1.54 to 1.48. When the rain stopped, with the effect of cracks, the rate of water infiltration was more prominent, which caused the safety factor to keep dropping even 2 days after the rain had ended. Meanwhile the trend was similar to the simulation without cracks.

5 Conclusion

Based on the above analysis and discussion, the following conclusions can be drawn:

(1) Red clay slopes are affected by the long-term wetting–drying cycles by climate variations, which make water content distribution more complex. The shallow layer of the slopes is sensitive to the external environments. The amount of change is related to the rainfall intensity.
(2) Due to the influence of the overburden pressure, the field-measured SWCCs vary at different depths, and the curves can be fitted by simple exponential equation.
(3) The SWCC of the laboratory test has an obvious hysteresis loop, the saturated water content is more than 40%, and an inflection point occurs when the water content is about 25%. The field SWCCs within 1 m below the surface of the red clay slope are almost among the hysteresis loop curves. The differences of results between laboratory and field derive from their different confinement condition.
(4) Due to low permeability of the red clay, the short-term rainfall has little impact on the slope stability, but the adverse effect sustained longer under continuous rainfall. The existence of cracks also facilitates rainwater infiltration leading to a decrease in slope stability.
(5) Different SWCCs were applied to the slope analysis, the law of water transport is different, but the depth of

the saturated zone is consistent. A safety factor analysis is conducted using the laboratory SWCC that is close to the result using the moisture wetting curves. When cracks are considered, the regulations are similar. And it is more conservative to choose the drying SWCC, which probably has certain reference value for the design of red clay slopes.

Acknowledgements This work was supported by the Science and Technology Foundation of Zhejiang Communications (Nos. 2014H13, 2017030) and the Fundamental Research Funds for the Central Universities (No. 2017M611674).

References

1. Au, S.W.C.: Rain-induced slope instability in Hong Kong. Eng. Geol. **51**(1), 1–36 (1998)
2. Crosta, G.: Regionalization of rainfall thresholds: an aid to landslide hazard evaluation. Environ. Geol. **35**(2), 131–145 (1998)
3. Dai, F.C.; Lee, C.F.: Frequency–volume relation and prediction of rainfall-induced landslides. Eng. Geol. **59**(3–4), 253–266 (2001)
4. Lim, T.T.; Rahardjo, H.; Chang, M.F.; Fredlund, D.G.: Effect of rainfall on matric suctions in a residual soil slope. Can. Geotech. J. **33**(4), 618–628 (1996)
5. Gasmo, J.M.; Rahardjo, H.; Leong, E.C.: Infiltration effects on stability of a residual soil slope. Comput. Geotech. **26**(2), 145–165 (2000)
6. Tsai, T.L.; Yang, J.C.: Modeling of rainfall-triggered shallow landslide. Environ. Geol. **50**(4), 525–534 (2006)
7. Ng, C.W.W.; Shi, Q.: A numerical investigation of the stability of unsaturated soil slopes subjected to transient seepage. Comput. Geotech. **22**(1), 1–28 (1998)
8. Chen, L.; Young, M.H.: Green-Ampt infiltration model for sloping surfaces. Water Resour. Res. **42**(7), 887–896 (2006)
9. Li, J.; Wang, Z.; Liu, C.: A combined rainfall infiltration model based on Green-Ampt and SCS-curve number. Hydrol. Process. **29**(11), 2628–2634 (2015)
10. Zhan, T.L.T.; Jia, G.W.; Chen, Y.M.; Fredlund, D.G.; Li, H.: An analytical solution for rainfall infiltration into an unsaturated infinite slope and its application to slope stability analysis. Int. J. Numer. Anal. Met. **37**(12), 1737–1760 (2013)
11. Leung, A.K.L.K.; et al.: Field monitoring of an unsaturated saprolitic hillslope. Can. Geotech. J. **48**(3), 339–353 (2011)
12. Li, A.G.; Yue, Z.Q.; Tham, L.G.; Lee, C.F.; Law, K.T.: Field-monitored variations of soil moisture and matric suction in a saprolite slope. Can. Geotech. J. **42**(1), 13–26 (2005)
13. Trandafir, A.C.; Sidle, R.C.; Gomi, T.; Kamai, T.: Monitored and simulated variations in matric suction during rainfall in a residual soil slope. Environ. Geol. **55**(5), 951–961 (2008)
14. Tu, X.B.; Kwong, A.K.L.; Dai, F.C.; Tham, L.G.; Min, H.: Field monitoring of rainfall infiltration in a loess slope and analysis of failure mechanism of rainfall-induced landslides. Eng. Geol. **105**(12), 134–150 (2009)
15. Pradel, D.; Raad, G.: Effect of permeability on surficial stability of homogeneous slopes. J. Geotech. Eng. **119**(2), 315–332 (1993)
16. Beldjelili, Y.; Tounsi, A.; Mahmoud, S.R.: Hygro-thermo-mechanical bending of S-FGM plates resting on variable elastic foundations using a four-variable trigonometric plate theory. Smart Struct. Syst. **18**(4), 755–786 (2016)
17. Attia, A.; Bousahla, A.A.; Tounsi, A.; Mahmoud, S.R.; Alwabli, A.S.: A refined four variable plate theory for thermoelastic analysis of FGM plates resting on variable elastic foundations. Struct. Eng. Mech. **65**(4), 453–464 (2018)
18. Song, Y.; Chae, B.; Lee, J.: A method for evaluating the stability of an unsaturated slope in natural terrain during rainfall. Eng. Geol. **210**, 84–92 (2016)
19. Zhang, J.; Jiao, J.J.; Yang, J.: In situ rainfall infiltration studies at a hillside in Hubei Province, China. Eng. Geol. **57**(1–2), 31–38 (2000)
20. Derbyshire, E.: Geological hazards in loess terrain, with particular reference to the loess regions of China. Earth Sci. Rev. **54**(1–3), 231–260 (2001)
21. Wu, L.Z.; Zhou, Y.; Sun, P.; Shi, J.S.; Liu, G.G.; Bai, L.Y.: Laboratory characterization of rainfall-induced loess slope failure. Catena **150**, 1–8 (2017)
22. Ng, C.W.W.; Pang, Y.W.: Influence of stress state on soil-water characteristics and slope stability. J. Geotech. Geonviron. **126**(2), 157–166 (2003)
23. Zhan, T.L.; Ng, C.W.; Fredlund, D.G.: Field study of rainfall infiltration into a grassed unsaturated expansive soil slope. Can. Geotech. J. **44**(44), 392–408 (2007)
24. Lemly, A.D.: Erosion control at construction sites on red clay soils. Environ. Manag. **6**(4), 343–352 (1982)
25. Xue, K.; Ajmera, B.; Tiwari, B.; Hu, Y.: Effect of long duration rainstorm on stability of Red-clay slopes. Geoenviron. Dis. **3**, 12 (2016)
26. Yuan, J.; He, Y.; Liu, J.: Construction of weak expansive red clay on Dongxin Expressway in Hunan Province, China. J. Perform. Constr. Fac. **30**(1), C4015001 (2015)
27. Meziane, M.A.A.; Abdelaziz, H.H.; Tounsi, A.: An efficient and simple refined theory for buckling and free vibration of exponentially graded sandwich plates under various boundary conditions. J. Sandw. Struct. Mater. **16**(3), 293–318 (2014)
28. Comegna, L.; Rianna, G.; Lee, S.; Picarelli, L.: Influence of the wetting path on the mechanical response of shallow unsaturated sloping covers. Comput. Geotech. **73**, 164–169 (2016)
29. Mukhlisin, M.; Baidillah, M.R.; Taha, M.R.; El-Shafie, A.: Effect of soil water retention model on slope stability analysis. Int. J. Phys. Sci. **6**(19), 4629–4635 (2011)
30. Antinoro, C.; Arnone, E.; Noto, L.V.: The use of soil water retention curve models in analyzing slope stability in differently structured soils. Catena **150**, 133–145 (2017)
31. Lumb, P.: Slope failures in Hong Kong. Q. J. Eng. Geol. Hydrog. **8**, 31–65 (1975)
32. Ng, C.W.W.; Pang, Y.W.: Influence of stress state on soil-water characteristics and slope stability. J. Geotech. Geoenviron. **126**(2), 157–166 (2000)
33. Liu, J.; Skoczylas, F.; Liu, J.: Experimental research on water retention and gas permeability of compacted bentonite/sand mixtures. Soil Found. **54**(5), 1027–1038 (2014)
34. Liu, J.; Ni, H.; Chen, Y.: Research on water retention and microstructure characteristics of compacted GMZ bentonite under free swelling conditions. Environ. Earth Sci. **7**(16), 583 (2018)
35. Liu, J.; Wu, Y.; Cai, C.; Ni, H.; Cao, X.; Pu, H.; Song, S.; Pu, S.; Skoczylas, F.: Investigation into water retention and gas permeability of Opalinus clay. Environ. Earth Sci. **77**(5), 213 (2018)
36. Van Genuchten, M.T.: A closed-form equation forpredicting the hydraulic conductivity of unsaturated soils. Soil Sci. Soc. Am. J. **44**, 892–898 (1980)
37. Liu, L.L.; Yin, K.L.: Analysis of rainfall infiltration mechanism of rainstorm landslide. Rock Soil Mech. **46**(4), 1061–1066 (2008)